

Benchmarking Variational Quantum Eigensolvers for Entanglement Detection in Many-Body Hamiltonian Ground States

Alexandre Drinko,^{1,*} Guilherme I. Correr,¹ Ivan Medina,^{1,2} Pedro C. Azado,¹ Askery Canabarro,^{1,3,4,5} and Diogo O. Soares-Pinto^{1,†}

¹*Instituto de Física de São Carlos, Universidade de São Paulo, CP 369, 13560-970 São Carlos, Brazil*

²*School of Physics, Trinity College Dublin, Dublin 2, Ireland*

³*Grupo de Física da Matéria Condensada, Núcleo de Ciências Exatas - NCEX,*

Campus Arapiraca, Universidade Federal de Alagoas, 57309-005 Arapiraca, Alagoas, Brazil

⁴*Department of Physics, Harvard University, Harvard University, Cambridge, Massachusetts 02138, USA*

⁵*Quantum Research Center, Technology Innovation Institute, Abu Dhabi, UAE*

Variational quantum algorithms (VQAs) have emerged in recent years as a promise to obtain quantum advantage. These task-oriented algorithms work in a hybrid loop combining a quantum processor and classical optimization. Using a specific class of VQA named variational quantum eigensolvers (VQEs), we choose some parameterized quantum circuits to benchmark them at entanglement witnessing and entangled ground state detection for many-body systems described by Heisenberg Hamiltonian, varying the number of qubits and shots. Quantum circuits whose structure is inspired by the Hamiltonian interactions presented better results on cost function estimation than problem-agnostic circuits.

I. INTRODUCTION

Variational quantum algorithms (VQAs) have been noticed as an interesting promise to achieve quantum advantage in the Noisy Intermediate Scale Quantum (NISQ) era of quantum computation [1–4]. Under the restrictions on the number of qubits and amount of noise in the contemporary quantum computers, quantum computing tasks that demand less qubits and low circuit depth are interesting to explore the limits of the available hardware [5].

The VQAs are hybrid task-oriented algorithms that combine quantum and classical computation to estimate a cost (or objective) function encoding the solution of a specific problem. While the quantum computer deals with the system state preparation, transformation, and measurements, the classical computer works with the outputs, post-processing an adjustable set of parameters imprinted in the system state by a parameterized quantum circuit [6, 7]. The chosen architecture of the circuit is usually termed *Ansatz* in this context and specifies the sequence of gates applied on the qubits. This hybrid loop is then repeated to optimize the chosen cost function [2, 5, 6, 8–10].

VQAs have been applied to solve a plethora of different tasks. In materials science, biology, and chemistry areas [11], they have been used to optimize molecular geometry [12] or find the ground state of molecular Hamiltonians [8], for example. VQAs also turned out to be an interesting tool for thermodynamics protocols, where we can mention the optimization of work extraction from quantum batteries [13, 14], preparation of thermal states [15–17], simulation of thermodynamic properties in met-

als [18] and study of many body features such as phase transitions [19]. Interestingly enough, VQAs also find applications outside of the natural sciences ground. In the realm of the financial market, for instance, VQAs have been used to solve problems involving portfolio optimization [20–22]. Other applications where VQAs are used alongside other classical and quantum machine learning methods can be found in [23–28].

Many of the first proposals for VQAs were built from inspiration in the problems of searching for ground states of molecules [10, 29]. This is a specific class of VQA, where the cost function takes the expectation value of the system’s Hamiltonian, named as Variational Quantum Eigensolver (VQE) [30, 31]. The VQE constitutes a powerful tool for studying the spectrum of interacting Hamiltonians [32–34], and maybe its most prominent application is the estimation of Hamiltonians ground states [30, 31], state preparations [35] and also entanglement detection in many body systems [36]. It is well known that entanglement constitutes an important resource for quantum computation [37, 38], quantum metrology [39] and quantum cryptography [40]. For bipartite quantum systems, there is a well-established approach to entanglement detection and quantification [41, 42]. However, for multipartite systems, methods for entanglement verification becomes a challenging problem where no unique manner to classify and quantify it is currently available [43]. For this reason, methods for entanglement detection and quantification are of utmost importance [44, 45]. Given this challenge, defining entanglement witnesses provides a practical method for detecting entanglement in experimental realizations [46–48].

In particular, the detection of entangled ground states in many body systems is an active topic of research that finds applications in a multitude of protocols [46, 49, 50]. In this work, we use the VQE to optimize an entanglement witness and detect entanglement in the ground

* adrinko@usp.br

† dosp@ifsc.usp.br

state of the Heisenberg Hamiltonian, which is an important Hamiltonian model for many body systems [51, 52]. Due to the availability of different quantum hardware where this task could be performed, each one having a different set of gates available for building the Ansatz, the main goal of our work is to benchmark some parameterized quantum circuits. To attain this task, we carefully analyze the performance of entanglement detection for each Ansatz by varying the number of qubits in the Heisenberg Hamiltonian and also the number of shots, which represents the number of measurement outcomes available to stochastically construct the cost function.

This work is organized as follows: In Sec. II we show the entanglement witness and the Hamiltonian used in all the simulations. In Sec. III a brief review of variational quantum eigensolvers is presented, followed by the Sec. IV where the parameterized quantum circuits are chosen for the benchmark. The results are presented in Sec. V where we compare the optimization process for different numbers of shots, the analysis of the entanglement detection and then the ground state convergence, highlighting the differences among the Ansätze and number of qubits. Finally in Sec. VI the discussion of some important aspects about the benchmarking and conclusions of the work.

II. HAMILTONIAN AS ENTANGLEMENT WITNESS

To detect the existence of entanglement we can use an entanglement witness, Z_{EW} , that represents a sufficient, but not necessary, criterion to detect entanglement [38, 43, 49, 50]. For each entangled state, exists at least one entanglement witness capable of detecting it [53].

An entanglement witness Z_{EW} is a Hermitian operator that gives a positive expectation value for all separable states and a negative for at least one entangled state:

$$\text{Tr}\{Z_{EW}\rho\} < 0, \quad \text{for at least one entangled } \rho, \quad (1)$$

$$\text{Tr}\{Z_{EW}\rho\} \geq 0, \quad \text{for all separable } \rho. \quad (2)$$

There is a plethora of methods to implement an entanglement witness by considering different criteria [43, 50]. We focus in Ref. [49], where it is presented how to witness entanglement in many body systems using the Hamiltonian as the entanglement witness. The separable states are in a convex set \mathcal{S} , such that there exists a minimum separable energy E_{sep} that corresponds to the lowest possible energy that a separable state can achieve,

$$E_{sep} = \min_{\rho_{sep} \in \mathcal{S}} \text{Tr}\{\rho_{sep} H\}. \quad (3)$$

If the ground state energy E_0 has a lower value than E_{sep} , we can define an entanglement gap $G = E_{sep} - E_0$, where all states for which the mean energy is inside the gap G are entangled. Then a Hamiltonian H has a non-zero entanglement gap if and only if no ground state of H is separable [49].

In this sense, every Hamiltonian H with a positive entanglement gap defines an energy-based entanglement witness

$$Z_{EW} \equiv H - E_{sep}\mathbb{1}, \quad (4)$$

that satisfies the Eqs. (1) and (2) for a set of entangled states bounded by the entanglement gap.

It is important to remark that the entanglement witness represents a sufficient but not necessary condition to detect entanglement. Then, if the witness application in a state results in a positive result, it does not imply the absence of entanglement, i.e., we have no information if the state is separable or entangled.

In this work, we choose the Heisenberg Hamiltonian with nearest-neighbour interaction,

$$H = -J \sum_{\langle i,j \rangle} (\sigma_x^{(i)} \sigma_x^{(j)} + \sigma_y^{(i)} \sigma_y^{(j)} + \sigma_z^{(i)} \sigma_z^{(j)}) + h \sum_i \sigma_z^{(i)}, \quad (5)$$

where J is the coupling constant, h is a external field and σ_i the Pauli matrices. This Hamiltonian was selected due to its wide applicability in diverse many-body systems as in quantum batteries [13, 54], describing Kagome lattices [55, 56], spin chains [51] and many-body localization [52].

III. VARIATIONAL QUANTUM EIGENSOLVER

As mentioned before the VQAs are task-oriented algorithms aimed to minimize a cost function that encodes the solution of the problem [7]. Usually, the cost function consists in the expectation value of an observable O , which codifies the problem of interest,

$$\mathcal{C}(\theta) = \text{Tr}\{OU(\theta)\rho_0 U^\dagger(\theta)\}, \quad (6)$$

where ρ_0 represents an input state. The cost function describes a hyper-surface in terms of the parameters θ and the optimization process will seek the global minimum of this cost landscape. The optimal parameters θ_{opt} represent the optimal solution codified in the observable O for a given Ansatz $U(\theta_{opt})$,

$$\theta_{opt} = \arg \min_{\theta} \text{Tr}\{OU(\theta)\rho_0 U^\dagger(\theta)\}, \quad (7)$$

which is expected to obtain a result close enough to the real solution.

This general framework shows the power of hybrid quantum-classical algorithms of this kind. A lot of problems that can be codified in a cost function of this type are potential candidates to be solved with VQAs. The cost function can be more general than the one posed in Eq. (6), but must at least be measurable in a quantum device. Some examples are the use of geometrical distance between states [57] or operators [58].

For our purposes, we chose the observable O , in Eq. (7), as the Hamiltonian (5). Then, our cost function

represents the average value of the Heisenberg Hamiltonian parameterized by the Ansatz $U(\theta)$. This case is a specific type of VQA named Variational Quantum Eigensolver (VQE) [29–31, 55, 59]. The cost function will be the mean energy value

$$\mathcal{C}(\theta) = \text{Tr}\{HU(\theta)\rho_0U^\dagger(\theta)\}, \quad (8)$$

where ρ_0 is the initial state. The main interest of the VQE is to find the minimum value of the cost function, that corresponds to the ground state energy. Once the cost function reaches the minimum, the optimized parameters, $\theta \rightarrow \theta_{\text{opt}}$, can be used to prepare the Hamiltonian ground state ρ_g ,

$$U(\theta \rightarrow \theta_{\text{opt}})\rho_0U^\dagger(\theta \rightarrow \theta_{\text{opt}}) \rightarrow \rho_g. \quad (9)$$

IV. ANSÄTZE CHOICE

The parameterized quantum circuit used in a VQA is the *Ansatz*. The Ansätze choice is an open problem in the proposal of methods and there are many consequences to the different options. Usually, this choice is heuristic and can either have motivation in the target problem or in the available hardware. A great diversity of Ansätze were proposed in literature to either general [6, 8, 60] or specific tasks [61, 62], motivating works testing the performance of each one of them in the implementation of VQAs [59, 63]. The selection of an Ansatz is therefore heuristic, so its choice may be motivated by the problem based on symmetries, the Hamiltonian of interest or entanglement [8, 9, 64].

Another reason to choose a specific Ansatz is the availability of the experimental platform and/or architecture of the quantum processor. In this section, we present the Ansätze that will be used in this work. To use the mean value of the entanglement witness (4) as cost function, we need two different types of Ansätze: one to search for the lowest separable energy E_{sep} and other to search for energy values lower than E_{sep} . This will configure the existence of an entanglement gap, i.e., the Hamiltonian have an entangled ground state.

One of the most used Ansätze is the Hardware Efficient Ansatz (HEA), which employ the repetition of rotation layers and entangling gates that could connect all the qubits based on the architecture of the available hardware. The main idea of this Ansatz is to minimize the circuit depth. The HEA is also used when there is a hardware limitation due to the experimental platform available, such as the qubit connectivity.

To find the lowest separable energy (see Sec.II), we propose a Hardware Efficient Separable Ansatz (HESA) where only local rotations, $(R_j^{(\kappa)}(\theta_\ell) = e^{-i\theta_\ell\sigma_j^{(\kappa)}/2})$, are performed in the qubits. the index $j = \{x, y, z\}$ denotes the axis of the rotation and κ the qubit in which the rotation is applied. The rotations selected for this Ansatz, Fig. 1, consists in the decomposition of a general unitary

acting in one qubit [65]. For a given initial separable state, the optimization process searches for the lowest energy separable eigenstate of the Hamiltonian in Eq. (5). The HESA is depicted in Fig. 1, where the initial state is fixed $|\psi_0\rangle = |0\rangle^{\otimes n}$, being n is the number of qubits.

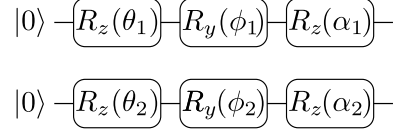


Figure 1: Hardware efficient separable Ansatz (HESA) for 2 qubits with only local rotations.

This first VQE process searches for the lowest separable energy, E_{sep} , to compose the energy-based entanglement witness. Scaling this Ansatz to more qubits will increase the number of trainable parameters in the same scale.

A. Hardware efficient Ansatz (HEA)

The class of hardware efficient Ansatz (HEA) is a broad set of circuits whose structure is problem-agnostic (its structure is not inspired on the studied problem) and its focus is to reduce the circuit depth. We selected two HEA circuits as presented in Fig. 2, based on single-qubit rotations and CNOT layers.

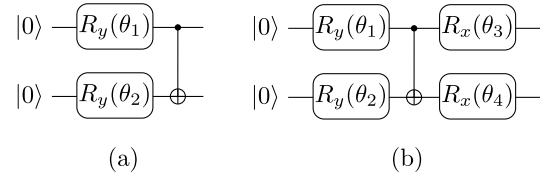


Figure 2: Hardware efficient Ansätze (HEA) for 2 qubits (a) one rotation and one CNOT layer HEA(a); (b) two rotation layers and one CNOT layer HEA(b).

Increasing the number of qubits, the Ansatz structure remains as a single rotation layer in each qubit, the CNOT layer applied sequentially in each pair of first neighbour qubits. The number of CNOT gates $\Lambda_{i,i+1}$ ($i = \text{control}$, $i + 1 = \text{target}$) in the Ansätze depicted in the Fig. 2 is $n - 1$, where n is the number of qubits,

$$U(\theta) = \prod_{i=1}^n R_y^{(i)}(\theta_i) \prod_{j=1}^{n-1} \Lambda_{j,j+1}, \quad (10)$$

for the HEA(a) and

$$U(\theta) = \prod_{i=1}^n R_x^{(i)}(\theta_i) \prod_{j=1}^{n-1} \Lambda_{j,j+1} \prod_{k=1}^n R_y^{(k)}(\theta_k), \quad (11)$$

for the HEA(b), where the difference between these Ansätze is the addition of a rotation layer $R_x^{(\cdot)}(\cdot)$. In both

cases of Fig. 2 we tried the simplest possible rotations, where the $R_y(\theta_i)$, Fig. 2 (a), presented the best results. Using different combinations of local rotations in Fig. 2 (b), we did not see a significant discrepancy among the results.

B. Sycamore-inspired Ansatz

Another selected Ansatz to the benchmark is inspired by Sycamore Google's chip [66, 67]. Its structure is described in [60] and is depicted in the Fig. 3. This Ansatz may be classified as HEA because its structure is fixed and problem agnostic. This Ansatz is built using local rotation gates, iSWAP and CPHASE for two qubits operations given by

$$i\text{SWAP}^\dagger(\theta) = \exp \left[-i\theta \left(\sigma_x^{(1)} \sigma_x^{(2)} + \sigma_y^{(1)} \sigma_y^{(2)} \right) \right], \quad (12)$$

$$\text{CPHASE}(\phi) = e^{-i\phi \sigma_z^{(1)} \sigma_z^{(2)}}, \quad (13)$$

and in this Ansatz, the initial state is prepared as an alternated product of $|0\rangle$ and $|1\rangle$.

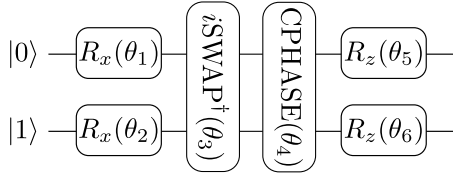


Figure 3: The Sycamore-inspired Ansatz for two qubits.

It is important to remark that the HEA have the drawback of not being efficient to some problems due to the lack of problem inspiration [68] and to the generation of great difficulty in training the cost function [7].

C. Hamiltonian Variational Ansatz (HVA)

The Hamiltonian Variational Ansatz (HVA) is inspired by one of the most famous VQA: the Quantum Alternating Operator Ansatz (QAOA) [26, 69], used mainly for combinatorial optimization problems. The QAOA consists in the alternated application of the circuit digitalization of the evolution of two non-commuting Hamiltonians: a Hamiltonian H_P in terms of products of the

Pauli- z matrices which encodes the problem of interest, and a Hamiltonian H_x in terms of products of Pauli- x matrices, to introduce coherences in the z -basis. This alternated application emulates the evolution of the total Hamiltonian $H = H_P + H_x$ via the Trotter-Suzuki decomposition [65]

$$e^{H_P+H_x} = \lim_{n \rightarrow \infty} (e^{H_P/n} e^{H_x/n})^n, \quad (14)$$

therefore, the unitary evolution of the system becomes

$$U = \lim_{n \rightarrow \infty} \prod_{k=1}^n e^{-iH_P t/n} e^{-iH_x t/n}. \quad (15)$$

The QAOA Ansatz is implemented by substituting the terms t/n with circuit parameters and taking the number of applications n to be of finite size instead, making the experimental implementation possible. The Ansatz is an approximation of the Trotter-Suzuki decomposition but it is still reliable. In fact, this restriction does not affect the possibility of building the desired state by the optimization of the parameters.

If, instead of two non-commuting terms, the Hamiltonian is decomposed in a bigger number of non-commuting terms, like in the Heisenberg Hamiltonian, $H = \sum_j H_j$, the Trotter-Suzuki decomposition reads

$$U \approx \prod_{k=1}^n \prod_j e^{-iH_j t/n}, \quad (16)$$

which is the decomposition for the HVA Ansatz. Each H_j represents one of the noncommuting terms.

Inspired by Refs. [9, 70], we split the couplings between qubits into even and odd links, thus each term will be of the form $H_{\kappa\kappa} = H_{\kappa\kappa}^{\text{odd}} + H_{\kappa\kappa}^{\text{even}}$. Exploiting the Heisenberg Hamiltonian symmetry, which has the same coupling constant J for each direction, we chose the parameterization such that the even links, odd links and individual terms of the external field have the same angles in each set. This decomposition for only one layer of the circuit will be in the form (omitting the state preparation)

$$U(\theta_1, \theta_2, \theta_3) \approx G(\theta_3, H_z) G(\theta_2, H_{yy}^{\text{even}}) G(\theta_2, H_{xx}^{\text{even}}) G(\theta_2, H_{zz}^{\text{even}}) G(\theta_1, H_{yy}^{\text{odd}}) G(\theta_1, H_{xx}^{\text{odd}}) G(\theta_1, H_{zz}^{\text{odd}}), \quad (17)$$

where $G(\theta, H) := e^{-i\theta H}$. The initial state is the ground

state of the sum of the even parts of the total Hamilto-

nian, i.e.,

$$|\psi_0\rangle = \bigotimes_{i=1}^{N/2} \frac{1}{\sqrt{2}} (|01\rangle - |10\rangle)_{2i-1, 2i}. \quad (18)$$

This is why the execution of the unitary is initialized with the odd part, so the initial state is not an eigenstate. Fig. 4 presents the state preparation and execution of HVA for a system with 4 qubits.

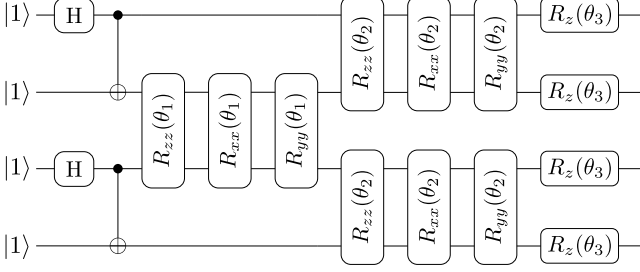


Figure 4: Structure of Hamiltonian Variational Ansatz (HVA) for 4 qubits.

The gates applied to one or two qubits are of the form

$$R_\alpha^{(j)}(\theta_\ell) = e^{-i\theta_\ell \alpha^{(j)}/2}, \quad (19)$$

where α is the Pauli strings (x, y, z, xx, xy, \dots) corresponding to the Pauli matrices and its products ($\sigma_x, \sigma_y, \sigma_z, \sigma_x \otimes \sigma_x, \sigma_x \otimes \sigma_y, \dots$) applied to the j qubit or pairs of qubits. For odd number of qubits, the remaining “not paired” qubit is connected with the others just by the first rotation layer.

D. Low-Depth Circuit Ansatz (LDCA)

The last selected Ansatz that we choose to benchmark is the low-depth circuit Ansatz presented in Ref. [67]. In Fig. 5 we depict this Ansatz for two qubits.

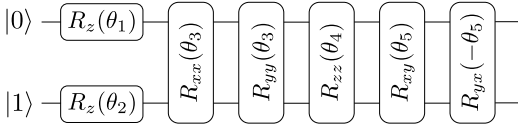


Figure 5: The Low-Depth Circuit Ansatz (LDCA) for two qubits.

This Ansatz was proposed in Ref. [71] with a similar structure where the Ansatz of Fig. 5 is a part of the decomposition of the complete LDCA.

Scaling the number of qubits, these operations are applied to all pairs of adjacent qubits (omitting the circuit θ parameters),

$$U(\theta) = \prod_{i=1}^{n-1} R_{yx}^{(i,j)} R_{xy}^{(i,j)} R_{zz}^{(i,j)} R_{yy}^{(i,j)} R_{xx}^{(i,j)} R_z^{(j)} R_z^{(i)}, \quad (20)$$

where $j = i + 1$.

V. RESULTS

In this section, we present the procedure and results from the Ansätze benchmark. As described in Sec. IV we need two Ansätze to perform the entanglement detection using the mean value of witness Eq. (4) as a cost function. For now on, we will take the coupling $J = -1$ and the absence of the external field $h = 0$ for all the simulations. Each Ansatz has a specific initial state, as depicted in each respective figure. For all the simulations we use the PennyLane library [72].

The first analysis was about the number of shots, then the entanglement detection, and finally the ground state convergence, varying the number of qubits. Each analysis considered all chosen Ansätze.

A. Number of Shots

The number of shots in a variational algorithm impacts cost function estimation. In an experimental context, the quantum hardware will run the circuit and perform the measurements in the σ_z basis in each wire of the circuit, i.e., in each qubit. This procedure, called shot, is repeated many times in order to obtain the relevant statistics of a certain observable, such as its mean value and variance. In the idealized scenario, an infinity number of measurements would be required to obtain the exactly observable quantities. Such infinity number of measurements is, however, impossible to do in practice.

To understand how the number of shots impact the cost function estimation, we ran our VQE simulations considering 10, 50, 100, and 300 shots. As the VQE simulation takes random initial parameters, and the initial conditions can strongly influence in the cost function convergence, we ran the VQE protocol 250 times for each fixed number of shots, each time taking a different set of initial random parameters. As an example, for the case with 10 shots, we proceed as follows. First, a random set of parameters is selected in the interval $[0, 2\pi]$. With this set, we collect 10 shots. Then, we proceed taking 10 shots in each iteration step. We verified that 200 interactions are good enough to make the cost function converge. After the convergence, we repeat these steps for another set of arbitrary initial parameters. We repeat this process 250 times, and finally compute the average cost function convergence. Moreover, we compare the average cost function using different number of shots with the average cost function obtained from the ideal case, i.e., the cost function analytically computed assuming that we have the complete information about the system’s state, which is given by $U(\theta)\rho_0 U^\dagger(\theta)$.

As presented in Fig. 6, we set a limit of 200 iterative steps to the VQE optimization. Most of the Ansätze (HEA(a), HEA(b), HVA) achieves a minimum value of 100 steps. The simulated VQE does not achieve the global minimum in these Ansätze. The LDCA will achieve the minimum in fewer steps, whereas Sycamore-

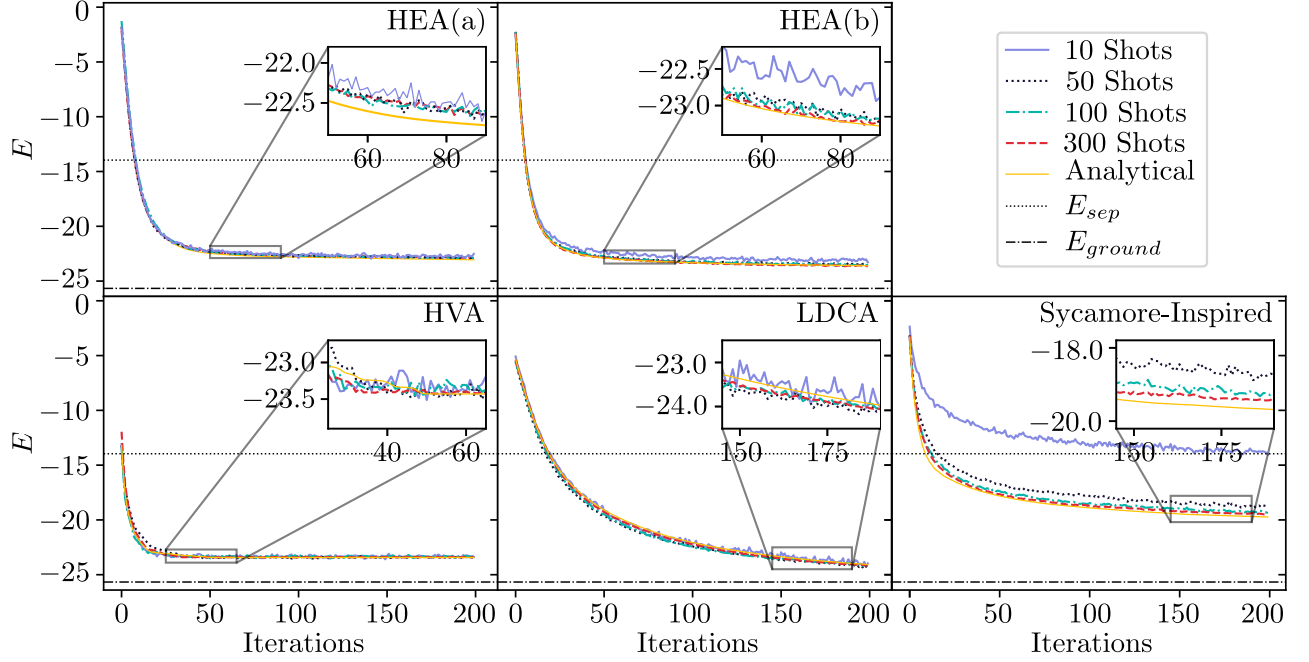


Figure 6: (Colour online) Optimization trajectory of ground state convergence for the HEA(a), HEA(b), HVA, LDCA and Sycamore-inspired Ansatzes. These curves are the mean value over 250 random starts with 15 qubits. The zoom was applied to visualize the proximity among different numbers of shots in each case. For 15 qubits $E_{sep} = -14$ and $E_{ground} = -25.6$

inspired needs even more steps to minimize the cost function. The Fig. 6 presents the mean value over 250 runs of each VQE. There are cases where the cost function reaches the global minimum (ground-state energy). On the other side, there are runs where the optimization gets imprisoned in a local minimum, leading the mean value to not achieve the global minimum.

The influence of shots in the Ansatzes HEA(a), HVA, and LDCA presents fluctuations close to the analytic calculation and the results are very close for all the shots presented in the Fig. 6. In the HEA(b) with 10 shots, there is a discrepancy in the mean value, where the optimization is worse than the other number of shots. The most affected case is for the Sycamore-inspired with 10 shots, where the entanglement witnessing criterion (Sec. VB) would occur after the 200 iterative steps. Increasing the number of shots, the optimization achieves better results, becoming closer to the analytic case.

As the optimization trajectory of the cost function has a similar behaviour to the analytic calculation (as we might see looking at the zoom in each Ansatz) for most of the presented cases, we chose to work with 100 shots.

B. Entanglement Detection

The entanglement detection: we run the VQE starting from the fixed state $|\psi_0\rangle = |0\rangle^{\otimes n}$ and optimize the parameters of HESA to search for the minimum separable energy E_{sep} . Using the other Ansatzes with entangling

gates, we run a second VQE to seek for energy values lower than E_{sep} , i.e., to detect entanglement using the witness presented in Eq. (4). In Fig. 7 we present the number of optimization steps needed to detect entanglement using the selected Ansatz from 2 to 15 qubits. As the initial set of parameters are randomly chosen (in the interval $[0, 2\pi]$), we run the optimization process 250 times to compute the mean number of steps needed to detect entanglement.

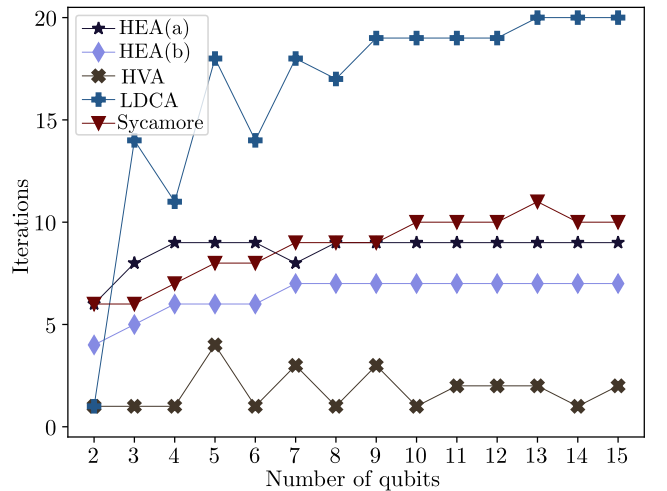


Figure 7: (Colour online) Iterations needed to detect entanglement using the energy-based entanglement witness for 2 to 15 qubits for each Ansatz.

We note in Fig. 7 that the entanglement detection occurs in a few optimization steps, where the LDCA needs more steps to detect entanglement compared to the other Ansätze. In HEA(a) the entanglement detection occurs in a few optimization steps and there is an improvement in HEA(b), where fewer steps are needed to detect entanglement. This is observed even when scaling the number of qubits. It is a very interesting case because both circuits have the same entanglement capability [73]. The one that needs fewer steps is the HVA, due to the initial state being prepared as presented in Eq. (18). Even for LDCA that demands more steps, all the Ansätze present an entanglement detection in a few optimization steps. So instead of setting a stop condition at entanglement detection, we let the VQE free to run until 200 optimization steps, to search for the entangled ground state.

C. Benchmark

As mentioned before, we run 250 random starts for each Ansatz to compute the mean value and the standard deviation. In Fig. 8 we present an example of the procedure for 6 qubits. The same was done by scaling the number of qubits.

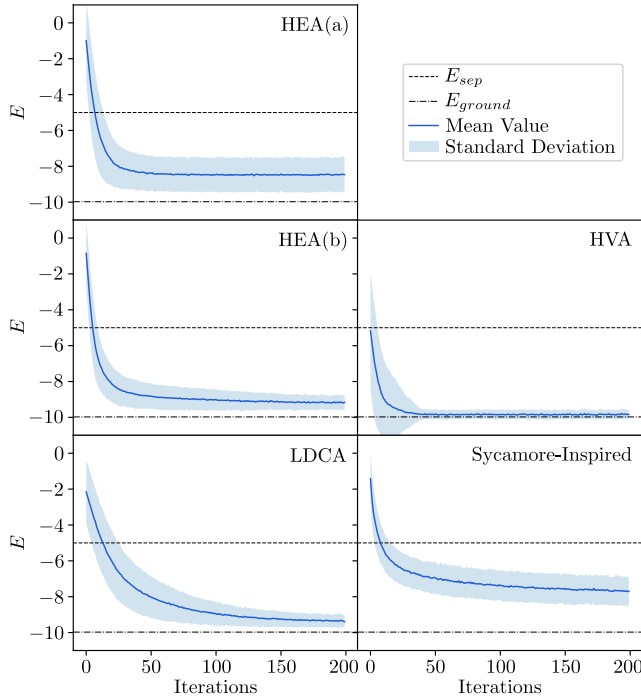


Figure 8: (Colour online) Ground state convergence and standard deviation over 250 random starts for the HEA(a) and (b), HVA, LDCA, and Sycamore-inspired Ansatz with 6 qubits. For 6 qubits we have $E_{sep} = -5$, and $E_{ground} = -9.9$.

Based on the Fig. 8, we note a large dispersion in standard deviation in HEA(a) that becomes narrow in HEA(b), this improvement occurs due to the additional

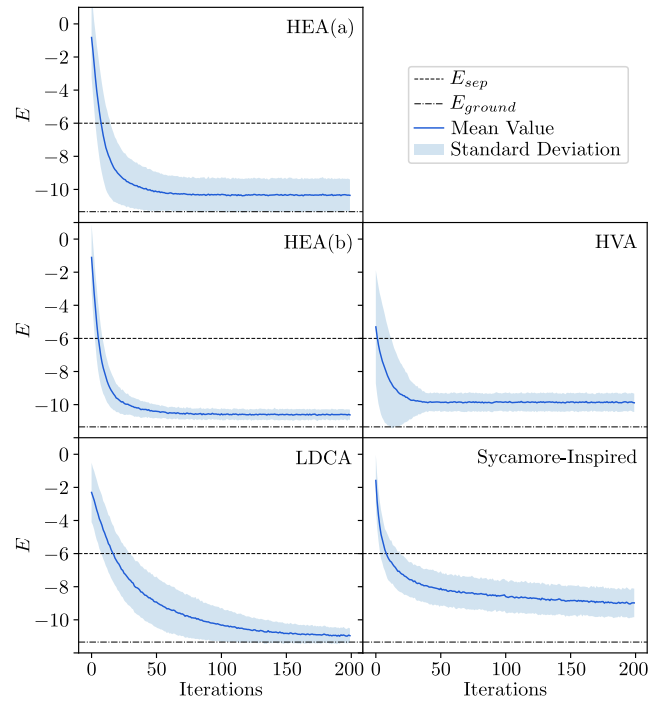


Figure 9: (Colour online) Ground state convergence and standard deviation over 250 random starts for the HEA(a) and (b), HVA, LDCA, and Sycamore-inspired Ansatz with 7 qubits. For 7 qubits we have $E_{sep} = -6$, and $E_{ground} = -11.3$.

rotation layer. Also, the mean value of the convergence gets closer to the ground state energy value. The best convergence to the entangled ground state is observed in HVA, followed by the LDCA. The Sycamore-inspired Ansatz needs more optimization steps to reach the ground state, spending a great computational time as the number of qubits increases.

In the HEAs, the convergence is better for an odd number of qubits as presented in Fig. 9, while the HVA has better convergence with an even number of qubits. The LDCA and Sycamore-inspired presented very similar behaviour in both cases.

VI. DISCUSSION AND OUTLOOK

Initially, our goal was to use the VQE with different Ansätze to witness ground state entanglement by using the energy as a part of the witness, where the Heisenberg Hamiltonian describes the many-body system. However, as presented in Sec. VB, the witnessing occurs in a few optimization steps. This is an important result, once this witnessing process could be used to verify the existence of an entangled ground state in more complex Hamiltonians. As described in Sec. II [49], if there is a state with an energy value lower than the minimum separable, it implies the existence of an entangled ground state. So,

instead of stopping the VQEs when the witnessing occurs, we search for the entangled ground state running the VQEs until 200 iterative steps.

After running for multiple qubits and shots choices, we decided to work with 100 shots. In Fig. 6 we present for 15 qubits these results as an example of this choice.

The Fig. 7 presents the number of iterations needed to witness entanglement, using the Eq. (4) for all the selected Ansätze where the number of qubits varies from 2 to 15. The many-body system is modelled with the Heisenberg Hamiltonian in the absence of external field (Eq. 5).

In Fig. 10 we present the ground state convergence normalized by the calculated ground state energy¹ for each Ansätze and number of qubits presented.

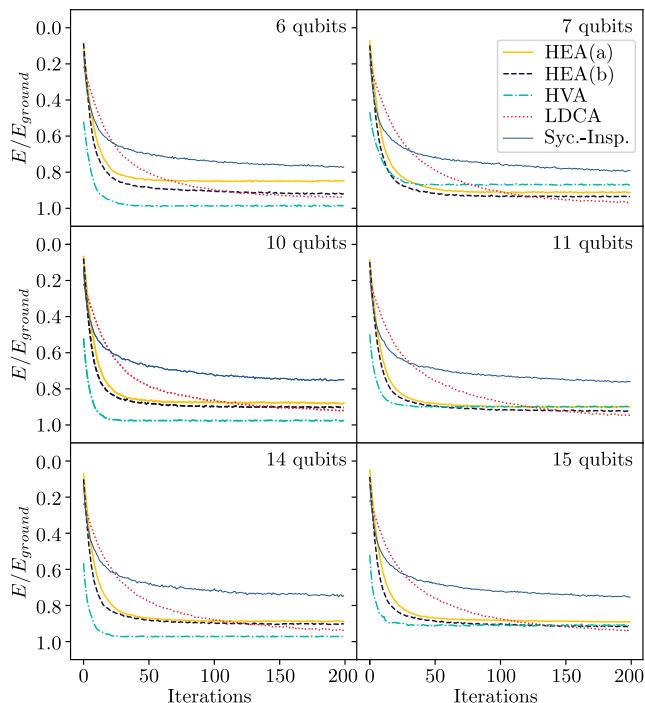


Figure 10: (Colour online) Mean value of ground state convergence normalized by the calculated ground state energy for all selected Ansätze and different numbers of qubits.

As the number of qubits increases, the number of trainable parameters also increases. This could lead to some optimization problems increasing the computational time or/and barren plateaus [6], which are regions in the cost landscape where the gradient vanishes, not giving a preferred path to the optimization process. In Table I we present the scale of trainable parameters associated with the number of qubits used in each Ansatz.

Looking at the ground state convergence, we show the mean value and standard deviation for 6 and 7 qubits

Ansatz	Number of parameters
HEA(a)	n_q
HEA(b)	$2n_q$
HVA	3
LDCA	$5n_q$
Sycamore-inspired	$6n_q$

Table I: Scale of trainable parameters associated to the number of qubits n_q for each Ansatz in a VQE process.

(Figs. 8 and 9). The HEA(a) presented a large dispersion in standard deviation. This possibly is associated with the concentration of local minima, observed in some optimization trajectories. Modifying the HEA(a) with an extra rotation layer we have HEA(b), where the optimization is improved. The dispersion is reduced and the mean value got closer to the ground state as we can see in Fig. 10. This improvement is observable for even and also odd numbers of qubits.

The HVA is an interesting case of a problem-inspired Ansatz where the gates are similar to the Hamiltonian interactions and before the parameterized quantum circuit there is a state preparation step. It was proposed in Ref. [9], where this Ansatz construction is to work with an even number of qubits, so the worst efficiency with odd qubits was expected, due to the last qubit not being connected to the other ones. This is the Ansatz that presents the best convergence (for an even number of qubits) in a few optimization steps and very narrow standard deviation. One interesting point about this Ansatz is the number of trainable parameters, that remain unchanged as the number of qubits is increased.

The LDCA presented a good performance to reach the ground state. However, by scaling the number of qubits, more iterative steps are needed to reach the ground state as we can see in Figs. 8, 9 and 10, where the standard deviation becomes narrower around 200 iterations. As the number of parameters increases with a factor of 5 of qubits, this Ansatz spends a great computational time to run.

Finally, the Sycamore-inspired Ansatz is the one we obtained the worst performance among the selected Ansätze. This is the Ansatz that spends the greatest number of optimization steps to obtain the ground state. This could be assigned to the scale of parameters that increase with a factor 6 of the number of qubits. The parameters scale, in certain cases, might improve the optimization task, for example increasing the number of layers. For our purposes with only one layer, this Ansatz is the one that needs more iterative steps to achieve a minimum.

It is important to remark that the VQAs structure consists of an Ansatz, cost function, and optimization process. In this paper we fixed the cost function and optimization method, just working with Ansätze changes. So the efficiency of each case could be changed by working with other VQA characteristics to obtain the best match

¹ The calculated value of ground state energy was found solving the Hamiltonian numerically.

of these aspects.

ACKNOWLEDGMENTS

This study was financed in part by the Coordenação de Aperfeiçoamento de Pessoal de Nível Superior – Brasil (CAPES) – Finance Code 001 (A.D. and G.I.C.). I.M. acknowledges financial support from São Paulo Research Foundation - FAPESP (Grants No. 2022/08786-2 and No. 2023/14488-7). P.C.A. acknowledges financial support from Conselho Nacional de Desenvolvimento Científico e Tecnológico - Brazil (CNPq - Grant No.

160851/2021-1). A.C. acknowledges a license by the Federal University of Alagoas for a sabbatical at the University of São Paulo, and partial financial support by CNPq (Grant No. 168785/2023-4), Alagoas State Research Agency (FAPEAL) (Grant No. APQ2022021000153), and São Paulo Research Foundation (FAPESP) (Grant No. 2023/03562-1). D.O.S.P. acknowledges the support by the Brazilian funding agencies CNPq (Grants No. 304891/2022-3 and No. 402074/2023-8), FAPESP (Grant No. 2017/03727-0) and the Brazilian National Institute of Science and Technology of Quantum Information (INCT/IQ).

-
- [1] John Preskill. Quantum computing in the nisq era and beyond. *Quantum*, 2:79, 2018.
 - [2] Frank Leymann and Johanna Barzen. The bitter truth about gate-based quantum algorithms in the nisq era. *Quantum Science and Technology*, 5(4):044007, 2020.
 - [3] Kishor Bharti, Alba Cervera-Lierta, Thi Ha Kyaw, Tobias Haug, Sumner Alperin-Lea, Abhinav Anand, Matthias Degroote, Hermann Heimonen, Jakob S. Kottmann, Tim Menke, Wai-Keong Mok, Sukin Sim, Leong-Chuan Kwek, and Alán Aspuru-Guzik. Noisy intermediate-scale quantum algorithms. *Rev. Mod. Phys.*, 94:015004, Feb 2022.
 - [4] Kishor Bharti, Alba Cervera-Lierta, Thi Ha Kyaw, Tobias Haug, Sumner Alperin-Lea, Abhinav Anand, Matthias Degroote, Hermann Heimonen, Jakob S Kottmann, Tim Menke, et al. Noisy intermediate-scale quantum algorithms. *Reviews of Modern Physics*, 94(1):015004, 2022.
 - [5] Adam Callison and Nicholas Chancellor. Hybrid quantum-classical algorithms in the noisy intermediate-scale quantum era and beyond. *Phys. Rev. A*, 106:010101, Jul 2022.
 - [6] Marco Cerezo, Andrew Arrasmith, Ryan Babbush, Simon C Benjamin, Suguru Endo, Keisuke Fujii, Jarrod R McClean, Kosuke Mitarai, Xiao Yuan, Lukasz Cincio, et al. Variational quantum algorithms. *Nature Reviews Physics*, 3(9):625–644, 2021.
 - [7] Marco Cerezo, Akira Sone, Tyler Volkoff, Lukasz Cincio, and Patrick J Coles. Cost function dependent barren plateaus in shallow parametrized quantum circuits. *Nature communications*, 12(1):1791, 2021.
 - [8] Abhinav Kandala, Antonio Mezzacapo, Kristan Temme, Maika Takita, Markus Brink, Jerry M. Chow, and Jay M. Gambetta. Hardware-efficient variational quantum eigensolver for small molecules and quantum magnets. *Nature*, 549(7671):242–246, September 2017.
 - [9] Roeland Wiersema, Cunlu Zhou, Yvette de Sereville, Juan Felipe Carrasquilla, Yong Baek Kim, and Henry Yuen. Exploring entanglement and optimization within the hamiltonian variational ansatz. *PRX Quantum*, 1:020319, Dec 2020.
 - [10] Jarrod R McClean, Jonathan Romero, Ryan Babbush, and Alán Aspuru-Guzik. The theory of variational hybrid quantum-classical algorithms. *New Journal of Physics*, 18(2):023023, feb 2016.
 - [11] Bela Bauer, Sergey Bravyi, Mario Motta, and Garnet Kin-Lic Chan. Quantum algorithms for quantum chemistry and quantum materials science. *Chemical Reviews*, 120(22):12685–12717, 2020.
 - [12] Alain Delgado, Juan Miguel Arrazola, Soran Jahangiri, Zeyue Niu, Josh Izaac, Chase Roberts, and Nathan Kibler. Variational quantum algorithm for molecular geometry optimization. *Physical Review A*, 104(5):052402, 2021.
 - [13] Ivan Medina, Alexandre Drinko, Guilherme I Correr, Pedro C Azado, and Diogo O Soares-Pinto. Variational-quantum-eigensolver-inspired optimization for spin-chain work extraction. *Physical Review A*, 110(1):012443, 2024.
 - [14] Duc Tuan Hoang, Friederike Metz, Andreas Thomasen, Tran Duong Anh-Tai, Thomas Busch, and Thomás Fogarty. Variational quantum algorithm for ergotropy estimation in quantum many-body batteries. *Phys. Rev. Res.*, 6:013038, Jan 2024.
 - [15] Guillaume Verdon, Jacob Marks, Sasha Nanda, Stefan Leichenauer, and Jack Hidary. Quantum hamiltonian-based models and the variational quantum thermalizer algorithm, 2019.
 - [16] Mirko Consiglio, Jacopo Settino, Andrea Giordano, Carlo Mastroianni, Francesco Plastina, Salvatore Lorenzo, Sabrina Maniscalco, John Goold, and Tony JG Apollaro. Variational gibbs state preparation on nisq devices. *arXiv preprint arXiv:2303.11276*, 2023.
 - [17] Ada Warren, Linghua Zhu, Nicholas J Mayhall, Edwin Barnes, and Sophia E Economou. Adaptive variational algorithms for quantum gibbs state preparation. *arXiv preprint arXiv:2203.12757*, 2022.
 - [18] Ana Clara das Neves Silva and Clebson Cruz. Simulating thermodynamic properties of dinuclear metal complexes using variational quantum algorithms, 2024.
 - [19] AV Uvarov, AS Kardashin, and Jacob D Biamonte. Machine learning phase transitions with a quantum processor. *Physical Review A*, 102(1):012415, 2020.
 - [20] Askery Canabarro, Taysa M. Mendonça, Ranieri Nery, George Moreno, Anton S. Albino, Gleydson F. de Jesus, and Rafael Chaves. Quantum finance: um tutorial de computação quântica aplicada ao mercado financeiro. *Revista Brasileira de Ensino de Física*, 44:e20220099, 2022.
 - [21] Shengbin Wang, Peng Wang, Guihui Li, Shubin Zhao,

- Dongyi Zhao, Jing Wang, Yuan Fang, Menghan Dou, Yongjian Gu, Yu-Chun Wu, et al. Variational quantum eigensolver with linear depth problem-inspired ansatz for solving portfolio optimization in finance. *arXiv preprint arXiv:2403.04296*, 2024.
- [22] Sebastian Brandhofer, Daniel Braun, Vanessa Dehn, Gerhard Hellstern, Matthias Hüls, Yanjun Ji, Ilia Polian, Amandeep Singh Bhatia, and Thomas Wellens. Benchmarking the performance of portfolio optimization with QAOA. *Quantum Information Processing*, 22(1), December 2022.
- [23] Chen-Yu Liu. Practical quantum search by variational quantum eigensolver on noisy intermediate-scale quantum hardware. *arXiv preprint arXiv:2304.03747*, 2023.
- [24] Vojtěch Havlíček, Antonio D Córcoles, Kristan Temme, Aram W Harrow, Abhinav Kandala, Jerry M Chow, and Jay M Gambetta. Supervised learning with quantum-enhanced feature spaces. *Nature*, 567(7747):209–212, 2019.
- [25] Jacob Biamonte, Peter Wittek, Nicola Pancotti, Patrick Rebentrost, Nathan Wiebe, and Seth Lloyd. Quantum machine learning. *Nature*, 549(7671):195–202, 2017.
- [26] Edward Farhi, Jeffrey Goldstone, and Sam Gutmann. A quantum approximate optimization algorithm, 2014.
- [27] Martín Larocca, Frédéric Sauvage, Faris M. Sbahi, Guillaume Verdon, Patrick J. Coles, and M. Cerezo. Group-invariant quantum machine learning. *PRX Quantum*, 3:030341, Sep 2022.
- [28] Isis Didier Lins, Lavínia Maria Mendes Araújo, Caio Bezerra Souto Maior, Plínio Marcio da Silva Ramos, Márcio José das Chagas Moura, André Juan Ferreira-Martins, Rafael Chaves, and Askery Canabarro. Quantum machine learning for drowsiness detection with eeg signals. *Process Safety and Environmental Protection*, 186:1197–1213, 2024.
- [29] Alberto Peruzzo, Jarrod McClean, Peter Shadbolt, Man-Hong Yung, Xiao-Qi Zhou, Peter J. Love, Alán Aspuru-Guzik, and Jeremy L. O’Brien. A variational eigenvalue solver on a photonic quantum processor. *Nature Communications*, 5(1), July 2014.
- [30] Jules Tilly, Hongxiang Chen, Shuxiang Cao, Dario Picozzi, Kanav Setia, Ying Li, Edward Grant, Leonard Wossnig, Ivan Rungger, George H Booth, et al. The variational quantum eigensolver: a review of methods and best practices. *Physics Reports*, 986:1–128, 2022.
- [31] M Cerezo, Kunal Sharma, Andrew Arrasmith, and Patrick J Coles. Variational quantum state eigensolver. *npj Quantum Information*, 8(1):113, 2022.
- [32] Oscar Higgott, Daochen Wang, and Stephen Brierley. Variational quantum computation of excited states. *Quantum*, 3:156, 2019.
- [33] Tyson Jones, Suguru Endo, Sam McArdle, Xiao Yuan, and Simon C Benjamin. Variational quantum algorithms for discovering hamiltonian spectra. *Physical Review A*, 99(6):062304, 2019.
- [34] Jin-Guo Liu, Yi-Hong Zhang, Yuan Wan, and Lei Wang. Variational quantum eigensolver with fewer qubits. *Phys. Rev. Res.*, 1:023025, Sep 2019.
- [35] Andrey Kerdashin, Alexey Uvarov, Dmitry Yudin, and Jacob Biamonte. Certified variational quantum algorithms for eigenstate preparation. *Physical Review A*, 102(5):052610, 2020.
- [36] Mirko Consiglio, Tony JG Apollaro, and Marcin Wieśniak. Variational approach to the quantum separability problem. *Physical Review A*, 106(6):062413, 2022.
- [37] Martin B Plenio and Shashank Virmani. An introduction to entanglement measures. *arXiv preprint quant-ph/0504163*, 2005.
- [38] Ryszard Horodecki, Paweł Horodecki, Michał Horodecki, and Karol Horodecki. Quantum entanglement. *Reviews of modern physics*, 81(2):865, 2009.
- [39] Pieter Kok, Samuel L Braunstein, and Jonathan P Dowling. Quantum lithography, entanglement and heisenberg-limited parameter estimation. *Journal of Optics B: Quantum and Semiclassical Optics*, 6(8):S811, 2004.
- [40] Dagmar Bruss and Chiara Macchiavello. Optimal eavesdropping in cryptography with three-dimensional quantum states. *Physical review letters*, 88(12):127901, 2002.
- [41] Barbara M Terhal. Bell inequalities and the separability criterion. *Physics Letters A*, 271(5-6):319–326, 2000.
- [42] Ryszard Horodecki, Michał Horodecki, and Paweł Horodecki. Teleportation, bell’s inequalities and inseparability. *Physics Letters A*, 222(1-2):21–25, 1996.
- [43] Nicolai Friis, Giuseppe Vitagliano, Mehul Malik, and Marcus Huber. Entanglement certification from theory to experiment. *Nature Reviews Physics*, 1(1):72–87, 2019.
- [44] F Shahandeh, J Sperling, and W Vogel. Structural quantification of entanglement. *Physical review letters*, 113(26):260502, 2014.
- [45] Mirjam Weilenmann, Benjamin Dive, David Trillo, Edgar A Aguilar, and Miguel Navascués. Entanglement detection beyond measuring fidelities. *Physical Review Letters*, 124(20):200502, 2020.
- [46] David Amaro and Markus Müller. Design and experimental performance of local entanglement witness operators. *Physical Review A*, 101(1):012317, 2020.
- [47] Jens Eisert, Fernando GSL Brandao, and Koenraad MR Audenaert. Quantitative entanglement witnesses. *New Journal of Physics*, 9(3):46, 2007.
- [48] Ke Wang, Weikang Li, Shibo Xu, Mengyao Hu, Jiachen Chen, Yaozu Wu, Chuanyu Zhang, Feitong Jin, Xuhao Zhu, Yu Gao, et al. Probing many-body bell correlation depth with superconducting qubits. *arXiv preprint arXiv:2406.17841*, 2024.
- [49] Mark R Dowling, Andrew C Doherty, and Stephen D Bartlett. Energy as an entanglement witness for quantum many-body systems. *Physical Review A*, 70(6):062113, 2004.
- [50] Otfried Gühne and Géza Tóth. Entanglement detection. *Physics Reports*, 474(1-6):1–75, 2009.
- [51] Shoji Yamamoto, S Brehmer, and H-J Mikeska. Elementary excitations of heisenberg ferrimagnetic spin chains. *Physical Review B*, 57(21):13610, 1998.
- [52] Marko Žnidarič, Tomaž Prosen, and Peter Prelovšek. Many-body localization in the heisenberg x x z magnet in a random field. *Physical Review B*, 77(6):064426, 2008.
- [53] Luigi Amico, Rosario Fazio, Andreas Osterloh, and Vlatko Vedral. Entanglement in many-body systems. *Reviews of modern physics*, 80(2):517, 2008.
- [54] Thao P Le, Jesper Levinsen, Kavan Modi, Meera M Parish, and Felix A Pollock. Spin-chain model of a many-body quantum battery. *Physical Review A*, 97(2):022106, 2018.
- [55] Jan Lukas Bosse and Ashley Montanaro. Probing ground-state properties of the kagome antiferromagnetic heisenberg model using the variational quantum eigensolver. *Physical Review B*, 105(9):094409, 2022.

- [56] Joris Kattemölle and Jasper Van Wezel. Variational quantum eigensolver for the heisenberg antiferromagnet on the kagome lattice. Physical Review B, 106(21):214429, 2022.
- [57] Bobak Toussi Kiani, Giacomo De Palma, Milad Marvian, Zi-Wen Liu, and Seth Lloyd. Learning quantum data with the quantum earth mover’s distance. Quantum Science and Technology, 7(4):045002, jul 2022.
- [58] Sumeet Khatri, Ryan LaRose, Alexander Poremba, Lukasz Cincio, Andrew T. Sornborger, and Patrick J. Coles. Quantum-assisted quantum compiling. Quantum, 3:140, May 2019.
- [59] Jiaqi Hu, Junling Li, Yanling Lin, Hanlin Long, Xu-Sheng Xu, Zhaofeng Su, Wengang Zhang, Yikang Zhu, and Man-Hong Yung. Benchmarking variational quantum eigensolvers for quantum chemistry, 2022.
- [60] Pierre-Luc Dallaire-Demers, Michał Stęchły, Jerome F Gonthier, Ntwali Toussaint Bashige, Jonathan Romero, and Yudong Cao. An application benchmark for fermionic quantum simulations. arXiv preprint arXiv:2003.01862, 2020.
- [61] Kazuhiro Seki, Tomonori Shirakawa, and Seiji Yunoki. Symmetry-adapted variational quantum eigensolver. Phys. Rev. A, 101:052340, May 2020.
- [62] Frederic Sauvage, Martin Larocca, Patrick J. Coles, and M. Cerezo. Building spatial symmetries into parameterized quantum circuits for faster training, 2022.
- [63] Alexandre Choquette, Agustin Di Paolo, Panagiotis Kl. Barkoutsos, David Sénéchal, Ivano Tavernelli, and Alexandre Blais. Quantum-optimal-control-inspired ansatz for variational quantum algorithms. Phys. Rev. Res., 3:023092, May 2021.
- [64] Alexandre Choquette, Agustin Di Paolo, Panagiotis Kl Barkoutsos, David Sénéchal, Ivano Tavernelli, and Alexandre Blais. Quantum-optimal-control-inspired ansatz for variational quantum algorithms. Physical Review Research, 3(2):023092, 2021.
- [65] Michael A. Nielsen and Isaac L. Chuang. Quantum Computation and Quantum Information: 10th Anniversary Edition. Cambridge University Press, 2011.
- [66] Frank Arute, Kunal Arya, Ryan Babbush, Dave Bacon, Joseph C Bardin, Rami Barends, Rupak Biswas, Sergio Boixo, Fernando GSL Brandao, David A Buell, et al. Quantum supremacy using a programmable superconducting processor. Nature, 574(7779):505–510, 2019.
- [67] Amara Katabarwa, Sukin Sim, Dax Enshan Koh, and Pierre-Luc Dallaire-Demers. Connecting geometry and performance of two-qubit parameterized quantum circuits. Quantum, 6:782, 2022.
- [68] Anbang Wu, Gushu Li, Yuke Wang, Boyuan Feng, Yufei Ding, and Yuan Xie. Towards efficient ansatz architecture for variational quantum algorithms, 2021.
- [69] Leo Zhou, Sheng-Tao Wang, Soonwon Choi, Hannes Pichler, and Mikhail D Lukin. Quantum approximate optimization algorithm: Performance, mechanism, and implementation on near-term devices. Physical Review X, 10(2):021067, 2020.
- [70] Wen Wei Ho and Timothy H. Hsieh. Efficient variational simulation of non-trivial quantum states. SciPost Phys., 6:29, 2019.
- [71] Pierre-Luc Dallaire-Demers, Jonathan Romero, Libor Veis, Sukin Sim, and Alán Aspuru-Guzik. Low-depth circuit ansatz for preparing correlated fermionic states on a quantum computer. Quantum Science and Technology, 4(4):045005, 2019.
- [72] Ville Bergholm, Josh Izaac, Maria Schuld, Christian Gogolin, Shahnawaz Ahmed, Vishnu Ajith, M Sohaib Alam, Guillermo Alonso-Linaje, B AkashNarayanan, Ali Asadi, et al. PennyLane: Automatic differentiation of hybrid quantum-classical computations. arXiv preprint arXiv:1811.04968, 2018.
- [73] Guilherme Ilário Correr, Ivan Medina, Pedro C Azado, Alexandre Drinko, and Diogo O Soares-Pinto. Characterizing randomness in parameterized quantum circuits through expressibility and average entanglement. arXiv preprint arXiv:2405.02265, 2024.